26th Conference on Severe Local Storms, American Meteorological Society, Nashville, TN, 5–8 Nov 2012

P87A USING A FOUR–FACE PHASED ARRAY RADAR TO DETECT TORNADOES AND MESOCYCLONES: A SIMULATION STUDY

Rodger A. Brown* and Vincent T. Wood
NOAA/National Severe Storms Laboratory, Norman, OK

1. INTRODUCTION

Phased array antennas, which have been used for military purposes since World War II (e.g., Visser 2005), are starting to be employed on research weather radars. Their basic feature is that they consist of thousands of transmit/receive elements. By phasing the sequence in which the elements radiate, the resulting *phased array radar* (PAR) beam is scanned electronically in azimuthal and vertical directions without moving the antenna [see, e.g., Zrnić et al. (2007) for an overview of the PAR]. This mode of beam scanning is in contrast with beams that are conventionally produced by mechanically steering a parabolic antenna.

In 2003, the National Weather Radar Testbed (NWRT) was established in Norman, Oklahoma to help evaluate, among other things, the operational potential of a phased array antenna as a future replacement for the parabolic antenna used by weather surveillance radars (e.g., Forsyth et al. 2003, Weber et al. 2007, Zrnić et al. 2007). The PAR being evaluated at the NWRT consists of a Weather Surveillance Radar–1988 Doppler (WSR–88D) transmitter and a single flat–face SPY–1 phased array antenna on loan from the U.S. Navy. This antenna consists of 4,352 elements that produce a half–power beamwidth (hereafter simply referred to as *beamwidth*) of 1.5° when the beam is perpendicular to the face and the beamwidth increases to 2.1° at a ±45° angle from the perpendicular. The antenna is rotated to cover the 90°–wide sector of interest and then remains stationary during data collection until the storms of interest move toward the edge of the sector. Since the electronic scanning of the antenna covers only one–quarter of the full 360°–wide azimuthal coverage region of a WSR–88D and since sophisticated electronic scanning techniques have been implemented, a volume scan within the 90°–wide sector can be completed in 1 min or less (e.g., Heinselman et al. 2008; Heinselman and Torres 2011).

If a phased array antenna eventually will replace the parabolic antenna on WSR–88Ds, a number of important decisions must be made, including the array configuration needed to cover 360° in azimuth and an acceptable beamwidth. For example, two possible configurations are discussed by Zhang et al. (2011), namely, a flat–face antenna and a cylindrical antenna. Zhang et al. also address the strengths and limitations of designs for dual polarization. A basic requirement from a meteorological perspective, however, is that the design does not adversely affect the current ability of National Weather Service (NWS) forecasters to resolve those evolving characteristics of severe storms that allow them to issue timely severe thunderstorm and tornado warnings. Since the flat–face antenna has a rather straightforward design, and that is the one being tested at the NWRT, we decided—as a preliminary study—to consider only that antenna design.

A basic characteristic of a flat–face phased array antenna is that the beamwidth increases as the beam electronically scans away from the broadside (or boresight) direction perpendicular to the face.[1] For narrow beams, like those used with weather radars, beamwidth (BW) changes in the azimuthal (vertical) direction according to

$$BW = BW_o / \cos\theta , \qquad (1)$$

where BW_o is the broadside beamwidth and θ is the azimuth (elevation) angle relative to the broadside direction (e.g., Visser 2005). For example, if one were to select three faces, the beam would scan ±60° horizontally from the broadside azimuth for each face. This means that

* *Corresponding author address*: Dr. Rodger A. Brown, National Severe Storms Laboratory, 120 David L. Boren Blvd., Norman, OK 73072; e-mail: Rodger.Brown@noaa.gov

[1] The term *broadside* comes from the old sailing warships where the cannons pointed perpendicular to the broad sides of the ship and fired coordinated “broadside” volleys.

the beamwidth at the transition azimuth of ±60° (BW_x) between faces would be twice the broadside beamwidth (BW_o). The ratios of BW_x to BW_o for this and several other face combinations are presented in Fig. 1. As indicated in the figure, there is minimal improvement in resolution (decrease in the BW_x/BW_o ratio) when more than four faces are used. Therefore, the most likely choice in the future would be to use four faces (where BW_x/BW_o = 1.414) in order to decrease the amount of beam broadening near the transitional azimuth. Each of the four antenna faces would be used to collect data in a 90°–wide volume scan in approximately 1 min; thus data would be collected over the full 360° using the four faces in only about 1 min compared to the 4–6 min required for WSR–88D data collection. In the remainder of this paper, we investigate the influence of beamwidth on the resolution of various–sized vortices while assuming that the simulated phased array radar has four faces.

2. METHOD

To investigate the influence of beamwidth on vortex detection, we scanned a simulated radar having a phased array antenna through the center of four nondivergent vortices representing tornadoes and mesocyclones. As shown in Table 1, peak tangential velocities of the vortices ranged from 25 to 100 m s^{-1} and the core diameters at which peak velocities occur ranged from 0.25 to 5.0 km. The Burgers–Rott vortex model (e.g., Davies–Jones 1986) was used to simulate tangential velocities within the vortices, where tangential velocity increased from zero at the center of the vortex to a broadly peaked maximum at the core radius and then decreased with increasing distance from the vortex center. This model is a good fit to Doppler velocity data collected by mobile Doppler radars near tornadoes (e.g., Bluestein et al. 2007; Tanamachi et al. 2007). For simplicity, vortex characteristics were assumed to be uniform with height and reflectivity was assumed to be uniform across the vortices.

For the Doppler radar computations, we used the radar simulator of Wood and Brown (1997). Instead of scanning with an antenna having a uniform beamwidth, we assumed that there were four phased array faces pointed toward the northeast, southeast, southwest, and northwest with the beam broadening along each face as the beam moved up to ±45° away from broadside azimuth. Since vortex resolution is a function of the beamwidth, we evaluated phased array antennas having broadside beamwidths of 0.5°, 0.75°, 1.0°, and 1.5°. The variation of beamwidth across all four faces for the four broadside beamwidths is shown in Fig. 2.

The radar beam was assumed to be one dimensional, consisting of only one range gate (range depth of 250 m) that scanned through the center of the vortex at an elevation angle of 0.5°. The main lobe of the beam was assumed to be Gaussian shaped with its full width being three times wider than the half–power beamwidth (e.g., Doviak and Zrnić 1993, chapter 7). The simulation did not include side lobes. Ordinarily, the mean Doppler velocity value at a given azimuth is computed from the signal returned from a given number of transmitted pulses. However, for the vortex simulations, we computed mean Doppler velocity at each azimuthal position from several hundred data points evenly spaced across the full one–dimensional main lobe centered on that azimuth.

For the simulated vortex measurements presented in the next section, vortices were placed at 1° increments across the 90°–wide azimuthal sector and at 1–km increments from 1 to 240 km from the radar, taking curvature of the earth into account. Each tornado (mesocyclone) was then scanned by the radar beam at 0.01° (0.02°) azimuthal increments, producing an azimuthal profile of mean Doppler velocity across the vortex. The resulting Doppler velocity signature of a vortex consists of a localized region of positive Doppler velocity values (flow away from the radar) near a localized region of negative Doppler velocity values (flow toward the radar) at the same range from the radar. For a mesocyclone, the average magnitude of the positive and negative peaks was computed, representing an approximation of the average peak tangential velocity at the core radius. For a tornado (following NWS convention), the Doppler velocity difference between the positive and negative peaks of the mean Doppler velocity profile was computed because the core diameter of the peak tornadic flow typically is smaller than the radar's beamwidth and thus not adequately resolved. The resulting tornadic vortex signature (TVS) is increasingly weaker than the tornado and the apparent core diameter is increasingly wider than the tornado with increasing distance from the radar (e.g., Brown et al. 1978).

3. RESULTS

The choice of broadside beamwidth as well as the increase in beamwidth away from the broadside direction affects vortex resolution. For example, in Fig. 3, each panel shows the ratio of the velocity difference of the extreme Doppler velocity values across the tornadoes (TOR) or the mean of the extreme values that approximate the peak rotational velocity of the mesocyclones (MESO) at a given azimuth relative to the value at the broadside azimuth. The values start to become degraded with increasing range as the beamwidth becomes as wide as the core diameter (curved dotted line). At farther ranges, the beamwidth is considerably wider than the core diameter and the amount of degradation becomes independent of core diameter or beamwidth (essentially constant ratios at a given azimuth). It is at these ranges that the signature of a tornado becomes a TVS with unresolvable tornado size or strength (e.g., Brown et al. 1978).

Since mesocyclones typically are at least an order of magnitude larger than tornadoes, they are considerably larger than the beamwidth and therefore do not suffer from as much degradation. However, the panels in Figs. 3 i–p show that mesocyclones can experience some degradation at farther ranges and with broader beamwidths. Since a TVS is evident immediately before and during the occurrence of a tornado and therefore does not provide much warning lead time, it is the strength and evolutionary characteristics of the parent mesocyclone that provide an average of 10–15 min of lead time for tornado warnings (e.g., Wurman et al. 2012). If a mesocyclone is crossing the transitional azimuthal region between antenna faces at a crucial time, it is important that the characteristics of the mesocyclone not be significantly degraded.

The data in Fig. 3 show the relative strengths of the rotation signatures across the face of the phased array antenna. However, the signatures themselves become weaker with increasing distance from the radar. This situation is illustrated in Fig. 4, where the apparent peak rotational velocities are compared to the actual peak rotational velocities of the tornadoes and mesocyclones listed in Table 1. Phased array broadside beamwidths of 1.5^{o} and 1.0^{o} result in weaker rotational velocities (shaded bands) than those detected by the super–resolution WSR–88D (dashed curves), while 0.75^{o} and 0.5^{o} beamwidths produce rotational velocities that are the same or stronger. The shaded band representing a broadside beamwidth of 0.75^{o} (increasing to 1.06^{o} across the face of the antenna) is coincident with and on the stronger side of the super–resolution curve (Figs. 4c, g, k, o). Therefore, a broadside beamwidth of 0.75^{o} provides at least the same detection capability as that for super–resolution WSR–88D sampling.

4. CONCLUDING DISCUSSION

The National Weather Radar Testbed in Norman, Oklahoma was established in part to evaluate the feasibility of eventually replacing the mechanically scanned parabolic antenna of the WSR–88D with an electronically scanned phased array antenna. With the detection of tornadoes and mesocyclones playing a vital decision role for NWS forecasters when issuing tornado and severe thunderstorm warnings, the choice of the number of antenna faces affects the detection capability of the radar. Since beamwidth increases inversely as the cosine of the azimuth angle from the broadside azimuth, the greater number of faces to cover the full 360^{o} in azimuth, the more uniform the beamwidth across a face. With a minimal improvement in resolution when more than four faces are used, the most likely choice in the future would be four faces, with each face covering a 90^{o} sector over which the beamwidth varies by a factor of 1.4.

Investigating the role of beamwidth on the detection of vortices, we used two simulated tornadoes and two simulated mesocyclones. A simulated phased array radar produced Doppler velocity signatures of the vortices across the full 90^{o}–wide sector covered by an individual antenna face out to ranges of 240 km. Since resolution decreases with increasing beamwidth, it is important to select a phased array antenna beamwidth that will provide at least the same tornado and mesocyclone resolution as the 1.0^{o} effective beamwidth provided by the WSR–88D at lower elevation angles with its mechanically steered parabolic antenna. A broadside beam-width of 0.75^{o} that increases to 1.06^{o} at the edge of the face provides such resolution.

If a decision is made that it is cost effective to replace the current antenna with phased array antennas, it would be approximately 2030 before the new antennas would become operational. A main consideration is the cost of the roughly 80,000 radiating elements and associated components that would be required for the phased

array antennas of each radar (e.g., National Research Council 2008). Industry partners have demonstrated that the cost of active PAR components is decreasing and current expectations are that the cost will be affordable by the time of deployment.

The NWS continues to add new technologies and capacities to the WSR–88D and any phased array radar system would have to meet or exceed these at the time of replacement. Current research and development activities are addressing the dual polarization requirement and future research and development will be addressing requirements imposed by the need of the radar to serve aviation as well as meteorological requirements.

Acknowledgments. We appreciate the helpful comments on this manuscript provided by Donald Burgess, Douglas Forsyth, Pamela Heinselman, and Sebastian Torres.

5. REFERENCES

Bluestein, H. B., C. C. Weiss, M. M. French, E. M. Holthaus, R. L. Tanamachi, S. Frasier, and A. L. Pazmany, 2007: The structure of tornadoes near Attica, Kansas, on 12 May 2004: High–resolution, mobile, Doppler radar observations. *Mon. Wea. Rev*., **135**, 475–506.

Brown, R. A., L. R. Lemon, and D. W. Burgess, 1978: Tornado detection by pulsed Doppler radar. *Mon. Wea. Rev.*, **106**, 29–38.

Brown, R. A., V. T. Wood, and D. Sirmans, 2002: Improved tornado detection using simulated and actual WSR–88D data with enhanced resolution. *J. Atmos. Oceanic Technol*., **19**, 1759–1771.

Davies–Jones, R. P., 1986: Tornado dynamics. *Thunderstorm Morphology and Dynamics*, 2nd ed., E. Kessler, Ed., University of Oklahoma Press, 197–236.

Doviak, R. J., and D. S. Zrnić, 1993: *Doppler Radar and Weather Observations*. 2nd ed., Academic Press, 562 pp.

Forsyth, D. E., and Coauthors, 2003: Building the National Weather Radar Testbed (phased–array). Preprints, *19th Intern. Conf. on Interactive Information and Processing Systems*, Long Beach, CA, Amer. Meteor. Soc., 2.8.

Heinselman, P. L., and S. M. Torres, 2011: High–temporal–resolution capabilities of the National Weather Radar Testbed phased–array radar. *J. Appl. Meteor. Climatol*., **50**, 579–593.

Heinselman, P. L., D. L. Priegnitz, K. L. Manross, T. M. Smith, and R. W. Adams, 2008: Rapid sampling of severe storms by the National Weather Radar Testbed phased array radar. *Wea. Forecasting*, **23**, 808–824.

National Research Council, 2008: Evaluation of the Multifunction Phased Array Radar Planning Process. National Research Council report, National Academy of Science, National Academies Press, 79 pp.

Tanamachi, R. L., H. B. Bluestein, W.–C. Lee, M. Bell, and A. Pazmany, 2007: Ground–based velocity track display (GBVTD) analysis of W–band Doppler radar data in a tornado near Stockton, Kansas, on 15 May 1999. *Mon. Wea. Rev*., **135**, 783–800.

Visser, H. J., 2005: *Array and Phased Array Antenna Basics*. John Wiley and Sons, 359 pp.

Weber, M. E., J. Y. N. Cho, J. S. Herd, J. M. Flavin, W. E. Benner, and G. S. Torok, 2007: The next–generation multimission U.S. surveillance radar network. *Bull. Amer. Meteor. Soc*., **88**, 1739–1751.

Wood, V. T., and R. A. Brown, 1997: Effects of radar sampling on single–Doppler velocity signatures of mesocyclones and tornadoes. *Wea. Forecasting*, **12**, 928–938.

Wurman, J., D. Dowell, Y. Richardson, P. Markowski, E. Rasmussen, D. Burgess, L. Wicker, and H. B. Bluestein, 2012: The second Verification of the Origin of Rotation in Tornadoes Experiment: VORTEX2. *Bull. Amer. Meteor. Soc*., **93**, 1147–1170.

Zhang, G., R. J. Doviak, D. S. Zrnić, R. Palmer, L. Lei, and Y. Al–Rashid, 2011: Polarimetric phased–array radar for weather measurement: A planar or cylindrical configuration? *J. Atmos. Oceanic Technol*., **28**, 63–73.

Zrnić, D. S., and Coauthors, 2007: Agile-beam phased array radar for weather observations. *Bull. Amer. Meteor. Soc*., **88**, 1753–1766.

Table 1. Maximum tangential velocity (V_{max}) and core diameter (CD) of two tornadoes and two mesocyclones used in the simulations. These values are a small sample of the wide range of tornado and mesocyclone characteristics.

Vortex	V_{max} (m s^{-1})	CD (km)
Tornado 1	100	0.25
Tornado 2	75	0.50
Mesocyclone 1	50	2.5
Mesocyclone 2	25	5.0

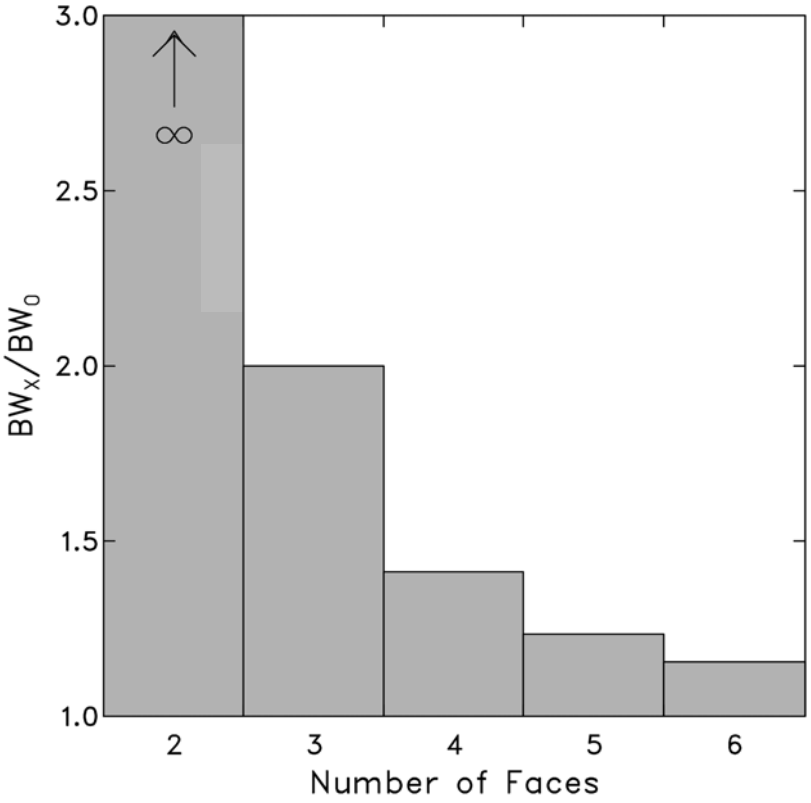

Fig. 1. Ratio of beamwidth at the transitional azimuth (BW_x) to the broadside beamwidth (BW_o) as a function of the number of faces used to encompass 360° of azimuth. The azimuthal coverage for each of 2, 3, 4, 5, and 6 faces is ±90°, ±60°, ±45°, ±36°, and ±30°, respectively. The use of 2 faces is unrealistic because the ratio is infinite owing to BW_x equaling BW_o /cos 90°.

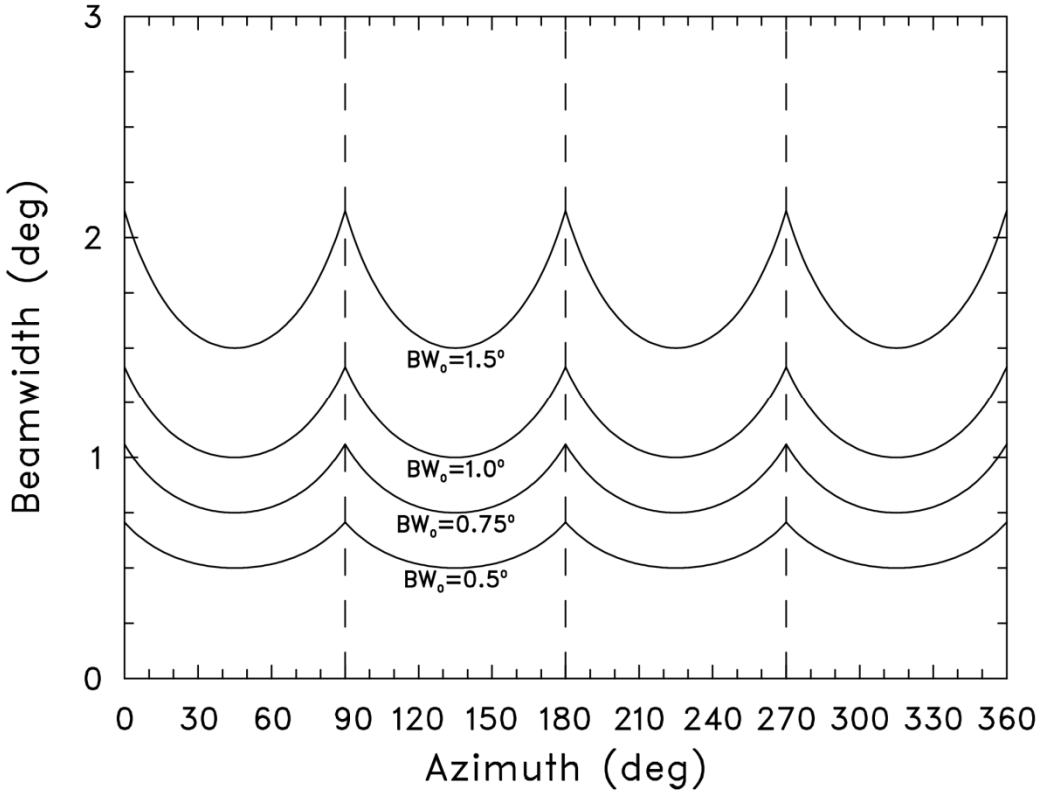

Fig. 2. Azimuthal variation of beamwidth for four different broadside beamwidths BW_o when using four phased array antennas arranged as a square (facing northeast, southeast, southwest, and northwest) for full azimuthal coverage of 360°. The vertical dashed lines mark the transitional azimuths between faces where BW_x = 1.414 BW_o. The variation ranges from 1.5° to 2.1° for a broadside beamwidth of 1.5° down to 0.5° to 0.71° for a broadside beamwidth of 0.5°.

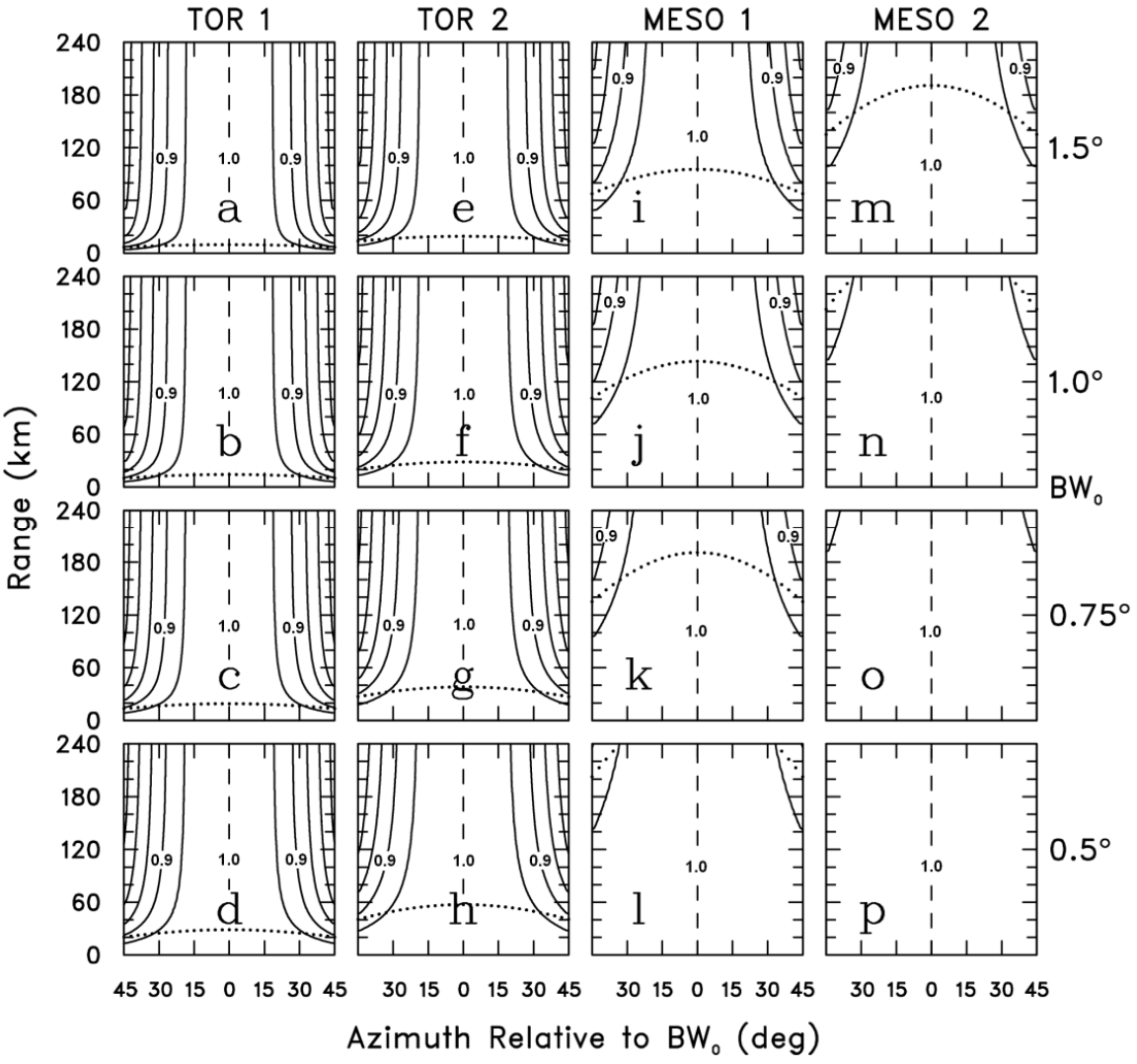

Fig. 3. Ratios of Doppler velocity differences associated with simulated tornadoes (a–h) and of peak rotational velocity signatures associated with simulated mesocyclones (i–p) relative to the simulated broadside values as a function of range and off–broadside azimuth angle for four broadside beamwidths (BW_o). Contour lines are at ratio intervals of 0.05. The curved dotted line indicates the range (R) at which the beamwidth is equal to the core diameter (CD) of the vortex as specified by $R = (57.296^o\ CD / BW_o) \cos(\theta)$.

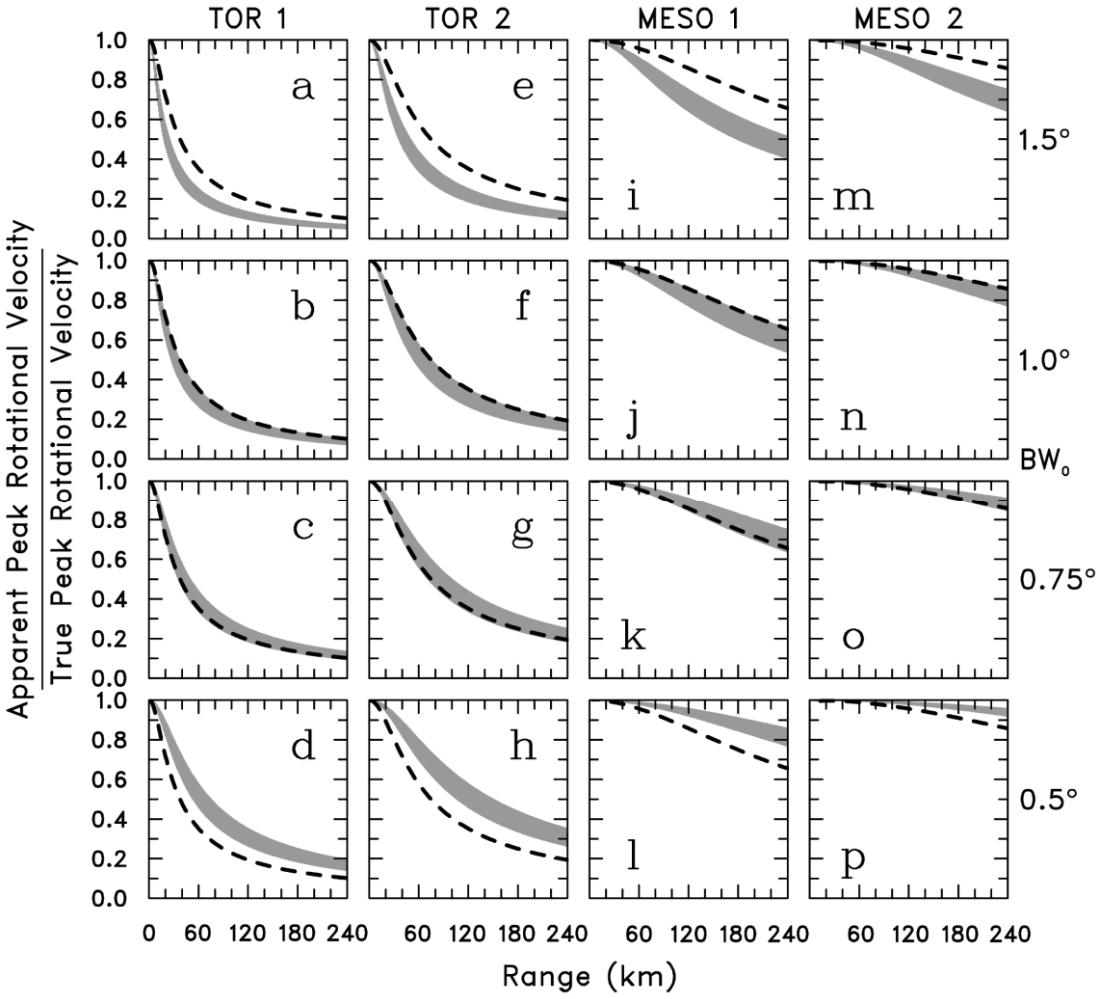

Fig. 4. Ratios of the apparent peak rotational velocity to the true peak rotational velocity for Tornadoes 1 and 2 and Mesocyclones 1 and 2 as a function of range and four broadside beamwidths (BW_o). For the tornadoes, the ratios are of velocity differences that produce the same ratios as if the mean rotational velocities had been used. The shaded band represents the spread of ratios between the azimuth angle at BW_o and the transitional azimuth angle of $\pm 45^o$. The dashed curve represents the WSR–88D super–resolution effective beamwidth of 1.0^o; the effective beamwidth is wider than the typical WSR–88D antenna beamwidth (about 0.9^o) because the antenna rotates during data collection (e.g., Doviak and Zrnić 1993, 193–197; Brown et al. 2002).